Cerebral Cortex, May 2019;29: 2051–2060

doi: 10.1093/cercor/bhy083
Advance Access Publication Date: 12 June 2018
Original Article

ORIGINAL ARTICLE

Prefrontal D1 Dopamine-Receptor Neurons and Delta Resonance in Interval Timing

Young-Cho Kim[1] and Nandakumar S. Narayanan[1,2]

[1]Department of Neurology, Carver College of Medicine, University of Iowa, Iowa City, IA 52242, USA and [2]Aging Mind and Brain Initiative, Carver College of Medicine, University of Iowa, Iowa City, IA 52242, USA

Address correspondence to Nandakumar Narayanan, 169 Newton Road, Pappajohn Biomedical Discovery Building, 1336, University of Iowa, Iowa City, IA 52242, USA. Email: Nandakumar-narayanan@uiowa.edu

Abstract

Considerable evidence has shown that prefrontal neurons expressing D1-type dopamine receptors (D1DRs) are critical for working memory, flexibility, and timing. This line of work predicts that frontal neurons expressing D1DRs mediate cognitive processing. During timing tasks, one form this cognitive processing might take is time-dependent ramping activity—monotonic changes in firing rate over time. Thus, we hypothesized the prefrontal D1DR+ neurons would strongly exhibit time-dependent ramping during interval timing. We tested this idea using an interval-timing task in which we used optogenetics to tag D1DR+ neurons in the mouse medial frontal cortex (MFC). While 23% of MFC D1DR+ neurons exhibited ramping, this was significantly less than untagged MFC neurons. By contrast, MFC D1DR+ neurons had strong delta-frequency (1–4 Hz) coherence with other MFC ramping neurons. This coherence was phase-locked to cue onset and was strongest early in the interval. To test the significance of these interactions, we optogenetically stimulated MFC D1DR+ neurons early versus late in the interval. We found that 2-Hz stimulation early in the interval was particularly effective in rescuing timing-related behavioral performance deficits in dopamine-depleted animals. These findings provide insight into MFC networks and have relevance for disorders such as Parkinson's disease and schizophrenia.

Key words: dopamine receptors, interval timing, prefrontal cortex, spike coherence, temporal control

Introduction

Medial and lateral regions of the mammalian frontal cortex are involved in cognitive processes such as working memory, flexibility, and timing (Fuster 2008). Frontal neurons encode intricacies of cognitive processing such as remembered items, prospective action, errors, goals, and temporal control of action (Niki and Watanabe 1979; Goldman-Rakic et al. 2004; Miller and D'Esposito 2005; Narayanan, Cavanagh, et al. 2013; Ma et al. 2014; Hardung et al. 2017). The coordinated activity of these neurons is detectable by macro-level techniques such as functional magnetic resonance imaging or electroencephalography (EEG). For instance, during tasks requiring cognitive control, frontal EEG electrodes often detect low-frequency oscillations in delta (1–4 Hz) and theta (4–8 Hz) frequency bands (Cavanagh and Frank 2014; Parker, Chen, et al. 2015; Parker et al. 2017; Chen et al. 2016; Kim et al. 2017).

Approximately 20% of frontal cortical neurons express D1-type dopamine receptors (Gaspar et al. 1995). In humans, positron emission tomography imaging studies have implicated D1DRs in working memory (Okubo et al. 1997; Abi-Dargham et al. 2002). In primates and rodents, local infusions of drugs targeting D1DRs impair performance on working memory, inhibitory control, flexibility, and timing tasks (Sawaguchi and Goldman-Rakic 1991, 1994; Vijayraghavan et al. 2007; St Onge et al. 2011; Parker, Alberico, et al. 2013; Parker, Ruggiero, et al. 2015; Jenni et al. 2017). D1DR agonists and antagonists can specifically attenuate neuronal activity related to working memory (Williams and Goldman-Rakic 1995; Vijayraghavan et al. 2007) and temporal processing (Narayanan et al. 2012; Parker, Andreasen, et al. 2013; Parker, Chen, et al. 2014, 2015; Parker, Ruggiero, et al. 2015; Narayanan 2016). During interval-timing tasks, this temporal processing can take

the form of "time-related ramping," which involves monotonic increases or decreases in neuronal firing rate across temporal intervals. Drugs acting on D1DRs specifically attenuate time-related ramping during interval-timing tasks (Parker, Chen, et al. 2014; Parker, Ruggiero, et al. 2015; Parker et al. 2017). Optogenetically inhibiting MFC D1DR+ neurons impairs interval timing (Narayanan et al. 2012). Finally, stimulating MFC D1DR+ neurons at 2 Hz but not 20 Hz can increase ramping activity and improve performance of interval-timing tasks (Kim et al. 2017). These data lead to the specific hypothesis that MFC D1DR+ neurons strongly exhibit time-related ramping activity.

We tested this hypothesis by using optogenetics to tag putative MFC D1DR+ neurons in D1-Cre mice during interval-timing tasks. To our surprise, we did not find evidence to support the hypothesis that a significant fraction of MFC D1DR+ neurons exhibited ramping activity. Instead, our data suggest that MFC D1DR+ neurons had delta/theta coherence with other MFC ramping neurons. Our findings could have relevance for our fundamental understanding of cortical networks and for human diseases involving impaired frontal dopamine.

Materials and Methods

Transgenic Mice

These experiments used identical procedures to our prior work (Kim et al. 2017). Briefly, we used mice in which Cre-recombinase was driven by the D1DR receptor promoter (*Drd1a-cre*$^{+}$; derived from Gensat strain EY262; aged 3 months; 25–32 g), or littermate controls. Mice were bred and verified by genotyping using primers for D1-Cre recombinase transgene (D1-Cre-F: AGG GGC TGG GTG GTG AGT GAT TG, D1-Cre-R: CGC CGC ATA ACC AGT GAA ACA GC). Mice consumed 1.5–2 g of food pellets (F0071, BioServ) during each behavioral session and additional food was provided 1–3 h after each behavioral session in the home cage. Single housing and a 12-h light/dark cycle were used. All experiments took place during the light cycle. Mice were maintained at approximately 85–90% of their free-access body weight during the course of these experiments for motivation. All procedures were approved by the Animal Care and Use Committee at the University of Iowa #4 071 105. A total of 6 mice were used for recording experiments (6 D1-Cre+ control mice for recording experiments with saline injected into the ventral tegmental area (VTA)). Eighteen separate mice were used for stimulation experiments: 6 control D1-Cre+ mice expressing ChR2 in the MFC with saline injected into the VTA, 6 D1-Cre+ mice expressing ChR2 in the MFC with mesocortical depletion, 6 control D1-Cre+ mice expressing control virus in the MFC.

Mice were trained to perform an interval-timing task with a 12-s interval according to methods described in detail previously (Kim et al. 2017). Briefly, operant chambers (MedAssociates) were equipped with a nose poke hole with a yellow light-emitting diode stimulus light (ENV-313 W), a pellet dispenser (ENV-203–20), and a house light (ENV-315 W). Behavioral arenas were housed in sound-attenuating chambers (MedAssociates). All behavioral responses including nose pokes and access to pellet receptacles were recorded with infrared sensors. First, animals learned to make operant nose pokes to receive rewards (20-mg rodent purified pellets, F0071, BioServe). After fixed-ratio training, animals were trained in a 12-s fixed-interval timing task in which rewards were delivered for responses after a 12-s interval. Early responses were not reinforced. Responses between 12 and 18 s resulted in trial termination with reward delivery. Rewarded nose pokes were signaled by a house light. The house light was turned on at reward delivery and lasted until the animal collected the reward. Each trial was followed by a 24 ± 6 s pseudorandom intertrial interval which concluded with an "on" nose poke hole light signaling the beginning of the next trial. All sessions were 60 min long.

Time-response histograms were normalized to total responses to investigate timing, independent of response rate. We calculated the "curvature" of time-response histograms by measuring the deviation from the cumulative distribution of a straight line (Fry et al. 1960). This metric is 0 with a flat time-response curve during interval and is closer to 1 when more responses are at 12 s and time-response histograms are more curved. Curvature has been used for over 50 years and in our past work to quantify interval-timing behavior (Fry et al. 1960; Narayanan et al. 2012; Parker, Chen, et al. 2014; Parker et al. 2017; Emmons et al. 2017; Kim et al. 2017). Curvature indices are higher with more "curved" time-response histograms. All behavioral data were tested for normality.

Mice trained in the 12-s interval-timing task were implanted with 16-channel 50 μm stainless-steel recording electrodes and an optical fiber in the MFC (Microprobes). Surgical procedures, neurophysiological recordings, neuronal analyses, and time-frequency analyses of mouse local field potential (LFP) were conducted identical to methods described in detail previously (Emmons et al. 2016; Kim et al. 2017; Parker et al. 2017).

Optogenetics

We used an Adeno-associated virus construct with floxed-inverted channelrhodopsin along with mCherry (UNC Viral Core; AAV5-EF-1a-DIO-hChR2(H134R)-mCherry; AAV-DIO-ChR2) (Cardin et al. 2009). Control virus expressed mCherry instead of ChR2. When delivered to transgenic D1-Cre+ mice, Cre recombination leads to high expression driven by an EF-1a promoter selectively in neurons expressing D1DRs. Mice were injected with AAV-DIO-ChR2 into the medial frontal cortex (MFC) (Mouse: AP: +1.8, ML: −0.5, DV: −1.5), with immediate placement of an optical fiber cannula (200 μm core, 0.22NA, Doric Lenses). The injection consisted of 0.5 μL of approximately 8 × 10^12 infectious particles per milliliter.

On testing days, D1-Cre+ mice with optical cannula were connected to the optical patch cable through a Zirconia ferrule (Doric Lenses) without anesthesia. Light was generated by a 473-nm DPSS laser source (OEM Laser Systems) and an optical rotary joint (Doric Lenses) was used to facilitate animal rotation during performance of the interval-timing task. During testing, each mouse performed the fixed-interval timing task for 1 h with light delivered at specific frequencies of stimulation. Specific frequencies of laser light were generated by transistor–transistor logic (TTL) signals sent through a microcontroller controlled by the operant behavior computer. In stimulation sessions, light was delivered from 0 to 6 s or 6 to 12 s during the fixed-interval at 0 and 2 Hz with a pulse width of 5 ms. Light stimulation was delivered on randomly selected trials (33% for each condition—early, late, and 0 Hz; 0 Hz meant that the laser was off and no laser light was delivered). The power output of the laser was adjusted to be 8 mW at the fiber tip before every experiment, power measurements verified that the laser reached 90% power within 0.74 ms of TTL triggers and maintained 8 mW with <5% error.

Neuronal Ensemble Recordings

Neuronal ensemble recordings in the MFC were made using a multielectrode recording system (Plexon). Raw signal was amplified with total gain of 5000 and high-pass filtered at 0.05 Hz and recorded with 16 bit resolution at 40 kHz sampling rate. To detect

spikes, raw signals were rereferenced using common median referencing to minimize potential non-neural electrical noises and band-pass filtered between 300 and 6000 Hz offline. Spikes were detected with a threshold of 5 median absolute deviations. Plexon Offline Sorter was used to sort single units and to remove artifacts. PCA and waveform shape were used for spike sorting. Spike activity was analyzed for all cells that fired at rates above 0.1 Hz. Statistical summaries were based on all remaining neurons. No subpopulations were selected or filtered out of the neuron database. Local field potential was recorded with band-pass filters between 0.05 and 1000 Hz. Analysis of neuronal activity and quantitative analysis of basic firing properties were carried out with custom routines for MATLAB. All behavioral events and laser triggers were recorded simultaneously using TTL inputs. Peri-event rasters and average histograms were constructed around trial start, and laser light pulse. For all analyses, statistical power was calculated using "sampsizepwr.m" in MATLAB.

In line with past work from our group, time-related ramping was defined using linear regression of firing rate binned at 0.1 s over the 12 s interval versus time (*fitlm.m* in MATLAB; Parker, Chen, et al. 2014; Parker, Ruggiero, et al. 2015; Narayanan 2016; Emmons et al. 2017; Kim et al. 2017; Parker et al. 2017). In addition, we used principal component analyses (PCA) to identify data-driven patterns of activity across neuronal ensembles as described in detail previously (Chapin and Nicolelis 1999; Narayanan and Laubach 2009; Parker, Ruggiero, et al. 2015; Emmons et al. 2017). Briefly, peri-event time histograms were constructed for each neuron over the 12-s interval for all trials, and singular value decomposition was computed across all neurons to calculate principal components (*pca.m* in MATLAB) for each neuron.

Spike–spike coherence was calculated between pairs of neurons recorded during the same sessions. The magnitude of the coherence for trial-aligned spike trains was calculated using the Chronux toolbox with multitaper Fourier analysis (Mitra and Bokil 2008). Calculations were performed using the following parameters: window size = 1 s; moving step = 0.1 s; number of tapers = 5. To compare across neurons with different firing rates, spike-rate differences are adjusted by estimating a correction factor that is conceptually equivalent to spike bootstrapping procedures (Aoi et al. 2015). Datasets and code are available at: https://narayanan.lab.uiowa.edu/article/datasets.

Histology

When experiments were complete, mice were anesthetized and sacrificed by injections of 100 mg/kg sodium pentobarbital. All mice were intracardially perfused with 4% paraformaldehyde. The brain was removed and postfixed in paraformaldehyde overnight, and immersed in 30% sucrose until the brains sank. About 50-μm sections were made on cryostat (Leica) and stored in PBS. Standard immunostaining procedures were performed in free-floating brain sections. Primary antibodies to Cre (mouse antiCre; Millipore-MAB 3120; 1:500), D1 receptor (rat antiD1 dopamine receptor; Sigma-D2944; 1:200), and tyrosine hydroxylase (rabbit antiTH; Millpore-AB152; 1:500) were incubated overnight at 4°C. Sections were visualized with Alexa Flour fluorescent secondary antibodies (goat antimouse IgG Alexa 633, goat antirat IgG Alexa 568, and goat antirabbit IgG Alexa 488; ThermoFisher; 1:1000) matched with the host primary by incubating for 2 h at room temperature. Images were captured on Leica SP5 laser scanning confocal microscope or Zeiss Apotome.2 Axio Imager.

Results

We trained 6 mice to perform a fixed-interval task with a 12-s interval (Fig. 1A). In these animals, we implanted optrodes targeting the MFC (Fig. 1B). We isolated 314 MFC neurons. We used optogenetic tagging to identify MFC D1DR+ neurons by recording from D1-Cre mice virally expressing AAV-DIO-ChR2 in the MFC, which expresses ChR2 in MFC D1DR+ neurons. Consistent with prior work 80 ± 2% of mCherry+ neurons had high levels of antiD1DR+ expression, and 20 ± 2% of mCherry+ neurons had low-levels of antiD1DR+ expression (Land et al. 2014). In recording experiments, MFC neurons that spiked within <5 ms of 473-nm laser onset were considered putative MFC D1DR+ neurons (Fig. 2). We identified 93 tagged MFC D1DR+ neurons. Optogenetic stimulation did not affect waveform shape (average correlation coefficient with nonstimulated spikes: $r = 0.99$). The average latency of tagged neurons was 1.99 ms and the jitter was 0.82 ms.

We also noticed that some MFC neurons had clear peaks in firing rate 6–18 ms after laser stimulation (Fig. 2B). This could be consistent with monosynaptic connectivity to MFC D1DR+ neurons. We operationally described these neurons as putatively connected with MFC D1DR+ neurons and termed them "D1DR+ Connected" neurons. About 149 MFC neurons met these criteria and were putatively labeled as D1DR+ Connected. Laser-induced spikes were more reliable in tagged D1DR+ neurons than in D1DR+ Connected neurons (0.30 ± 0.02 vs. 0.14 ± 0.008, $t_{(471)} = 8.003$, $P < 0.0001$; statistical power = 0.99; Fig. 2C). Because of limitations in our recording techniques, it is difficult to make further conclusions about the anatomical or synaptic configuration of these neurons. In the remaining 72 neurons, we could identify no discernable change in spike rate with optogenetic stimulation. These neurons were labeled as "untagged." D1DR+ neurons had similar firing rates to D1DR+ Connected and untagged neurons (D1DR+: 8.4 ± 1.2 Hz; D1DR+ Connected: 7.9 ± 0.9 Hz; Untagged: 9.8 ± 1.3 Hz).

We explored how MFC D1DR+ neurons, MFC D1DR+ Connected neurons, and untagged MFC neurons were involved in interval timing. Past work by our group and others (Narayanan et al. 2012; Xu et al. 2014; Gouvea et al. 2015; Parker, Ruggiero, et al. 2015; Emmons et al. 2017; Kim et al. 2013, 2017) has identified 3 common patterns of MFC activity: stimulus-related activity (Fig. 3A), temporal processing in the form of time-related ramping activity (Fig. 3B), and response-related activity (Fig. 3C). Time-related ramping was defined as a monotonic increase or decrease in firing rate as quantified by linear regression of firing rate over the interval (Parker, Chen, et al. 2014; Parker, Ruggiero, et al. 2015; Narayanan 2016; Emmons et al. 2017; Kim et al. 2017; Parker et al. 2017). These

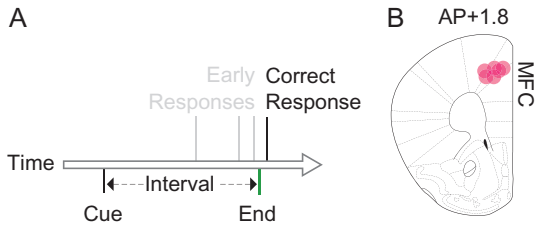

Figure 1. Interval timing requires mesocortical dopamine. (A) We trained mice to perform a fixed-interval timing task, in which rodents had to make a motor response 12 s after a starting cue. Early responses were not reinforced, whereas the first response after interval end was rewarded. (B) We recorded from 6 mice with optrodes placed in medial frontal cortex (MFC; red dots).

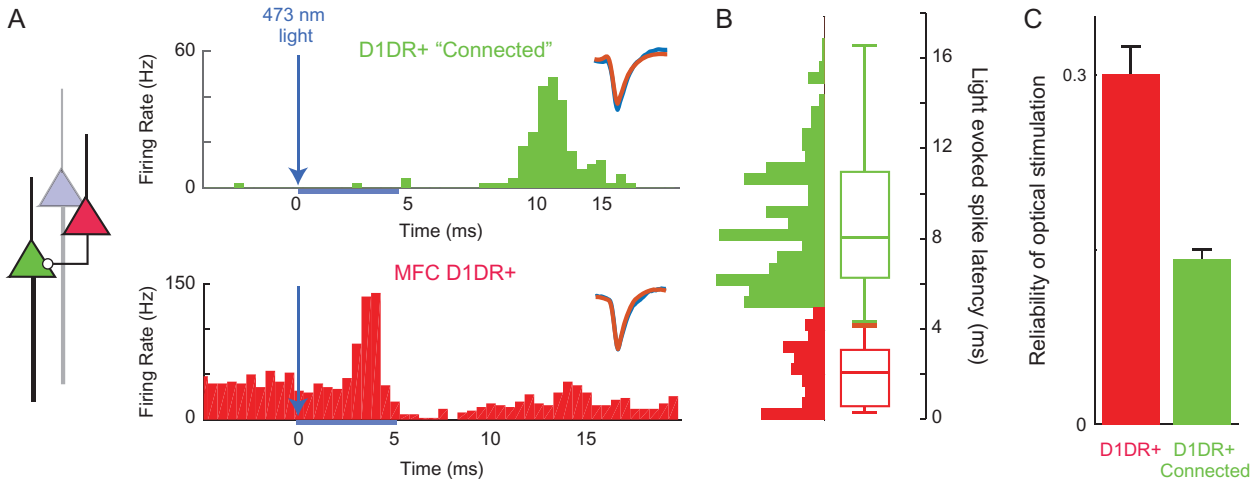

Figure 2. Optogenetic tagging of MFC D1DR+ and connected neurons. (*A*) By virally expressing DIO-ChR2 in the MFC of D1-Cre mice, we can optogenetically "tag" MFC D1DR+ neurons (in red) as those with short-latency action potentials <5 ms from 473-nm laser onset, as this latency is most consistent with action potentials initiated within the recorded neuron rather than synaptic transmission. Aside from tagged neurons, however, we noticed a second peak in latency in some neurons that could be consistent with monosynaptic connectivity to MFC D1DR+ neurons. We operationally termed neurons with this peak MFC D1DR+ "Connected" neurons (in green). (*B*) Light-evoked latencies as histograms and box plots of putative MFC D1DR+ (red) and putative MFC D1DR+ Connected neurons are shown. Waveforms for nonstimulated (orange) and stimulated trials (blue) inset. (*C*) The reliability of action potentials triggered by optical stimulation pulse is significantly higher in D1DR+ neurons than D1DR+ connected neurons. * indicates $P < 0.05$.

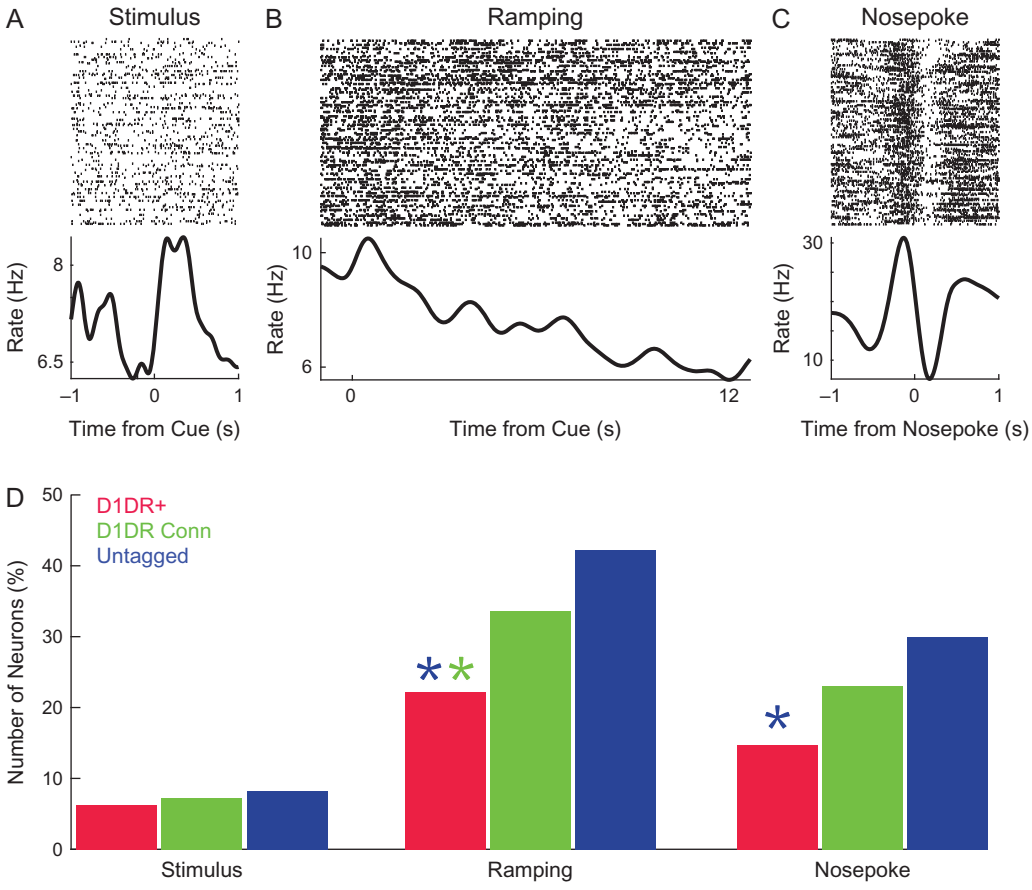

Figure 3. MFC D1DR+ neurons have less time-related ramping than MFC neurons. Examples of (*A*) a stimulus-modulated neuron, (*B*) a neuron with time-related ramping, and (*C*) a nose poke-modulated neuron. (*D*) We examined the number of significantly modulated MFC D1DR+ neurons (red), MFC D1DR+ Connected neurons (green), and untagged MFC neurons (blue). There were less MFC D1DR+ ramping neurons than MFC D1DR+ Connected (green asterisk) and untagged MFC neurons (blue asterisk). There were also fewer MFC D1DR+ than untagged MFC nose poke neurons (blue asterisk). Data from 314 MFC neurons in 6 mice, including 93 MFC D1DR+ neurons. * indicates $P < 0.05$.

studies have demonstrated that MFC D1DR pharmacological or optogenetic manipulation can selectively influence ramping, leading to our hypothesis that MFC D1DR+ neurons ramp.

We found that 21 of 93 MFC D1DR+ neurons (23%) exhibited time-related ramping (5 ramped up; 16 ramped down). To our surprise, this was significantly less than MFC D1DR+ Connected neurons (51 of 149; 34%; $\chi^2 = 3.7$, $P < 0.05$; statistical power = 0.89; 25 ramped up and 26 ramped down) and significantly less than untagged MFC neurons (31 of 72, or 43%; χ^2=7.9 $P < 0.005$; statistical power = 0.97; 8 ramped up, 23 ramped down; Fig. 3D). There were similar fractions of stimulus-related activity in MFC D1DR+ neurons and untagged neurons (Fig. 3D). These data indicate that MFC D1DR+ neurons had "less" time-related ramping than other populations of MFC neurons. We also found that MFC D1DR+ neurons had less motor-related activity than untagged MFC neurons ($\chi^2 = 5.7$, $P < 0.02$; Fig. 3D), but not less than MFC D1DR+ Connected neurons.

To further analyze patterns of MFC neurons, we turned to a data-driven method, PCA. This method makes no assumptions about the underlying structure of the data, but simply tries to minimize variance by rotating multivariate data along orthogonal basis functions. We have used PCA extensively in the past to capture patterns of neuronal activity (Chapin and Nicolelis 1999; Narayanan and Laubach 2009; Parker, Chen, et al. 2014; Emmons et al. 2017; Kim et al. 2017; Parker et al. 2017). PCA revealed that the first 4 components each accounted for >10% of variance among MFC ensembles, with PC1 accounting for 22% of variance and PC4 accounting for 11% of variance (Fig. 4A–C). Smaller components >PC5 accounted for progressively less variance and were not analyzed. In line with past work, PC1 exhibited a monotonic change over the interval, which we interpret as time-related ramping (Narayanan and Laubach 2009; Narayanan 2016; Kim et al. 2017; Parker et al. 2017). PC1 had significantly less loading on MFC D1DR+ neurons than untagged neurons ($t_{(163)} = 3.6$, $P < 0.0004$; statistical power = 1; Fig. 4C) or MFC D1DR+ Connected neurons ($t_{(240)} = 2.1$, $P < 0.03$; statistical power = 0.99; Fig. 4C). MFC D1DR+ neurons loaded strongly on PC4. This was stronger for MFC D1DR+ neurons than untagged neurons ($t_{(163)} = 2.0$, $P < 0.05$) and MFC D1DR+ Connected neurons ($t_{(240)} = 2.3$, $P < 0.02$). Thus, 2 methods with vastly different analytical approaches (linear regression and PCA) indicated that MFC D1DR+ neurons had less time-related ramping than untagged MFC neurons. These results do not support the hypothesis that MFC D1DR+ neurons exhibit ramping more strongly than MFC D1DR+ Connected or untagged MFC neurons.

Consequently, we investigated alternative patterns of MFC D1DR+ activity. Several prior studies by our group have indicated that low-frequency delta/theta rhythms around 4 Hz require MFC D1DRs (Cavanagh and Frank 2014; Parker, Narayanan, et al. 2014; Parker, Chen, et al. 2015; Parker, Ruggiero, et al. 2015; Chen et al. 2016). Accordingly, we examined spike-to-spike coherence between MFC D1DR+ neurons and D1DR+ Connected neurons as well as untagged neurons (Fig. 5A). We found that MFC D1DR+ neurons had prominent cue-locked delta/theta coherence with ramping D1DR+ Connected neurons (Fig. 5A). This was significantly more than we observed with nonramping D1DR+ Connected neurons and untagged MFC neurons (Fig. 5B–E; delta: $t_{(778)} = 2.4$, $P < 0.02$—statistical power = 0.82; theta; $t_{(778)} = 2.7$, $P < 0.008$—statistical power = 0.93; beta; $t_{(778)} = 0.5$, $P < 0.60$). These data indicate that MFC D1DR+ neurons could have specific cue-triggered delta/theta synchrony with ramping neurons. We also noticed that this interaction was strongest early in the interval between 0 and 6 s at 1–8 Hz (Fig. 5F; paired $t_{(250)} = 2.9$, $P < 0.004$ first 6 s–last 6 s; statistical power = 0.83). These findings suggest that MFC D1DR+ neurons might interact with MFC ramping neurons via delta/theta interactions early in the interval.

To test the behavioral significance of these interactions, we optogenetically stimulated MFC D1DR+ neurons at delta frequencies (2 Hz) early versus late in the interval. Our prior work indicates that MFC D1DR+ stimulation for the entire 12-s interval could compensate for behavioral deficits of dopamine depletion (Kim et al. 2017). Data in Fig. 5F predict that stimulation should have different effects in the interval, with the first 6 s being more effective as delta interactions are stronger earlier in the interval. To test this prediction, we stimulated MFC D1DR+ neurons from 0 to 6 s (early) and from 6 to 12 s (late) at

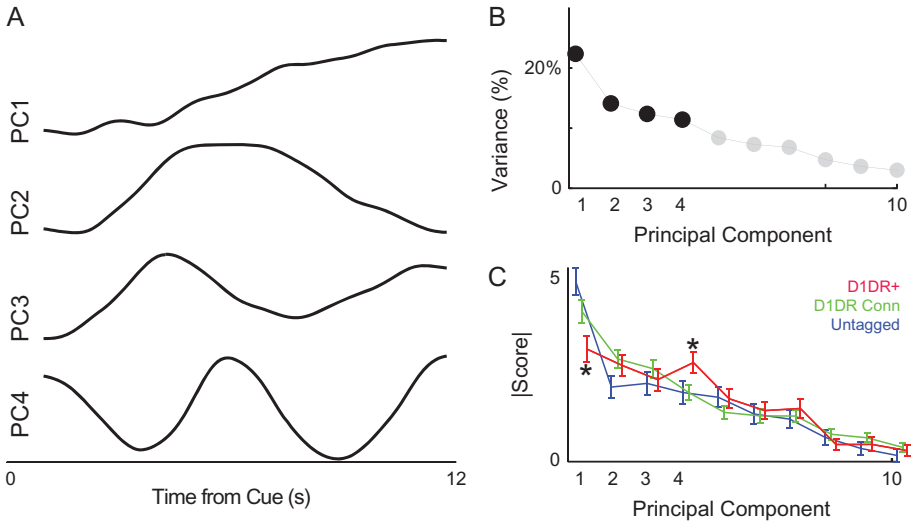

Figure 4. MFC D1DR+ neuronal ensembles have distinct principal components, including less ramping activity. Principal component analysis is a data-driven approach to identify dominant patterns in multivariate data. (A) Four large components were noted; as in past work, PC1 was a "ramping" component and PC4 had an oscillatory pattern with a period of approximately 6 s. (B) The first 4 PCs each explained >10% of variance. (C) MFC D1DR+ neurons had less loading on PC1 and more loading on PC4. Data from 314 MFC neurons, including 93 MFC D1DR+ neurons, in 6 mice. * indicates $P < 0.05$ for MFC D1DR+ versus untagged MFC neurons.

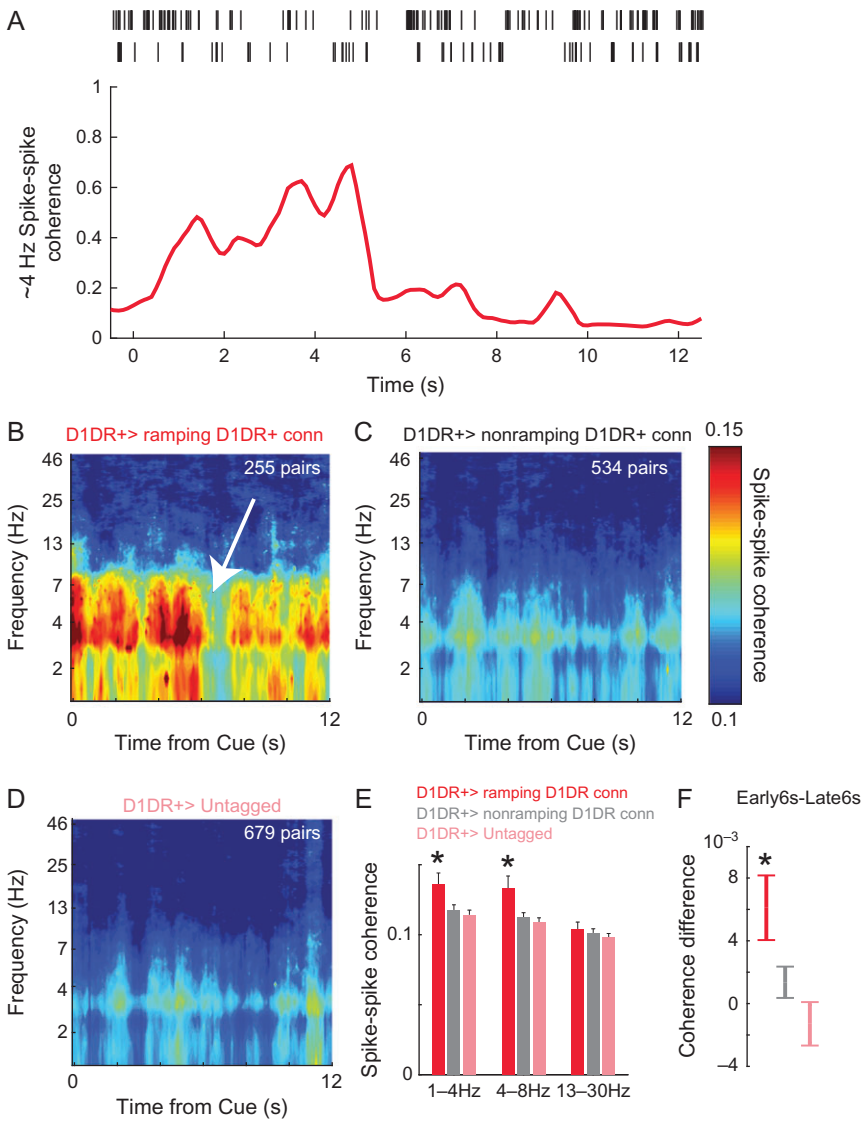

Figure 5. MFC D1DR+ neurons have delta/theta coherence with connected ramping neurons. (*A*) We examined spike–spike coherence, which involves frequency and phase-specific synchrony between the spike trains of 2 neurons. For example, these 2 MFC neurons had high approximately 4-Hz spike–spike coherence early in the interval, implying that they had more spikes with frequency/phase synchrony at approximately 4 Hz. Later in the delay, this pair had less approximately 4-Hz spike–spike coherence. (*B*) MFC D1DR+ neurons had marked cue-triggered delta/theta coherence that was prominent early in the interval (white arrow appears to be a point of transition). This pattern was not apparent with nonramping Connected neurons or with untagged MFC neurons. (*E*) In addition, MFC D1DR+ neurons had stronger coherence with connected ramping neurons than with nonramping or untagged neurons. (*F*) MFC D1DR+ neurons had significantly more coherence early in the interval compared with late in the interval (see white arrow in (*B*) where a transition at approximately 6 s is apparent). Note that in *B–D*, the scale was adjusted to best visualizes coherence between MFC D1DR+ neurons and ramping neurons, and the number of pairs going into each comparison appears in white at the top right. Data from 4679 combinations of 93 D1DR+ neurons, 149 D1DR+ Connected neurons, and 72 untagged MFC neurons in 6 mice. * indicates $P < 0.05$.

delta frequencies (2 Hz, delivering a total of 12 laser pulses early/late in the interval; Fig. 6A), which would exogenously drive delta coherence among MFC D1DR+ neurons. We measured interval-timing performance by the "curvature" of time-response histograms during behavior. This measure is based on the cumulative distribution of time-response histograms and is independent of overall response rate. Values range between 0 and 1, with impaired performance leading to flatter curvature values closer to 0 (Fry et al. 1960; Narayanan et al. 2012; Parker, Chen, et al. 2014; Kim et al. 2017). Consistent with our previous studies, we found no effects in mice with intact mesocortical dopamine circuits (Fig. 6A). However, these mice are likely at maximal performance, thus limiting this experiment by a ceiling effect (Vijayraghavan et al. 2007; Cools and D'Esposito 2011; Narayanan, Rodnitzky, et al. 2013; Kim et al. 2017). To explore if MFC D1DR+ stimulation was effective in animals with interval-timing deficits, we depleted dopamine in the VTA using the neurotoxin 6OHDA, which impairs interval timing (VTA-Saline: 0.19 ± 0.06 vs. VTA-6OHDA: 0.07 ± 0.08; $t_{(11)} = 3.3$, $P < 0.01$; statistical power = 0.88). For these VTA-6OHDA animals, there were differential effects of 2-Hz stimulation early versus late in the interval ($t_{(5)} = 6.2$, $P < 0.002$; Fig. 6B). Stimulation early in the interval was sufficient to improve interval timing and rescue timing deficits in these animals (early 6 s vs. nonstim: $t_{(17)} = -2.6$, $P < 0.02$). The minimum time animals started responding was 6.6 s; thus, optogenetic

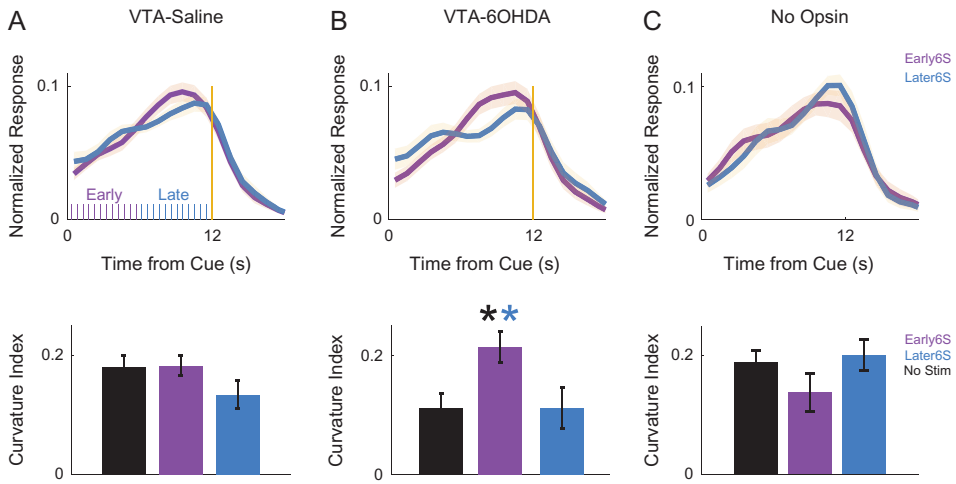

Figure 6. MFC D1DR+ delta stimulation early in the interval can rescue deficits in VTA-6OHDA animals. Time-response histograms for (*A*) VTA-Saline animals (purple ticks indicate laser stimulation pulses early in the interval, blue ticks indicate laser stimulation pulses late in the interval), (*B*), VTA-6OHDA animals, and (*C*) a separate group of 6 control D1-Cre mice expressing virus but no opsin. Blue—MFC D1DR+ 2 Hz stimulation late in the delay from 6 to 12 s; Purple—stimulation from 0 to 6 s. Data from 18 mice. * indicates $P < 0.05$.

stimulation in the early epoch from 0 to 6 s occurred prior to any responses made by the mice. Notably, there was no effect on mean-response times (VTA-Saline: nonstim −9.7 ± 0.3, early 6 s −9.6 ± 0.3, later 6 s −9.7 ± 0.3; VTA-6OHDA: nonstim − 9.8 ± 0.2, early 6 s −9.7 ± 0.3, later 6 s −10.1 ± 0.4) or overall accuracy (VTA-Saline: nonstim − 20 ± 1%, early 6 s −22 ± 1%, later 6 s −22 ± 1%; VTA-6OHDA: nonstim −21 ± 1%, early 6 s −25 ± 2%, later 6 s −23 ± 2%). No effects were found in control sessions with mCherry in D1-Cre mice (Fig. 6C). These data support the idea that cue-triggered delta coherence between D1DR+ neurons and ramping neurons early in the interval is key for interval-timing performance.

Discussion

We tested the hypothesis that frontal D1DR+ neurons strongly exhibited time-related ramping, a key temporal signal, during interval timing. We recorded from optogenetically tagged MFC D1DR+ neurons and connected neurons as rodents performed an interval-timing task. While approximately 23% of MFC D1DR + neurons exhibited ramping activity, this was less than we observed among other MFC neurons. As such, our data did not provide evidence to support our hypothesis. However, we found that MFC D1DR+ neurons had cue-triggered delta coherence with connected ramping neurons that was strongest early in the interval, predicting that optogenetically increasing delta coherence among these neurons would affect interval-timing performance. In line with this idea, 2-Hz stimulation of MFC D1DR+ neurons early in the interval compensated for behavioral deficits caused by mesocortical dopamine depletion. These data replicate previous studies from our group manipulating, recording from, and stimulating MFC D1DR+ neurons (Parker, Chen, et al. 2014; Parker, Ruggiero, et al. 2015; Kim et al. 2017). The present study provides novel information that (a) MFC D1DR+ neurons do not strongly exhibit ramping activity, (b) MFC D1DR+ neurons are strongly coherent with MFC ramping neurons early in the interval, and (c) stimulating MFC D1DR + early in the interval is sufficient to compensate for behavioral deficits caused by disrupting mesocortical dopamine. This line of work suggests that MFC D1DR+ neurons provide input to MFC ramping neurons via delta/theta interactions early in the interval. This interaction provides insight into how MFC D1DR+ neurons might support cognitive processing.

Modulation of delta/theta frequencies in MFC represent the need for cognitive control (Cavanagh et al. 2012; Narayanan, Cavanagh, et al. 2013; Cavanagh and Frank 2014; Chen et al. 2016). These signals depend on cortical D1DRs and are attenuated in human patients with schizophrenia and Parkinson's disease (Parker, Chen, et al. 2015; Kim et al. 2017; Parker et al. 2017) as well as in rodent models (Parker, Chen, et al. 2015; Kim et al. 2017; Parker et al. 2017). During interval timing, the need for cognitive control is triggered by the cue, which initiates temporal processing (Buhusi and Meck 2005; Meck et al. 2008). In fixed-interval timing tasks, the cue functions as a reward-predictive CS+ involving phasic dopamine release from midbrain dopamine neurons (Schultz 1997; Fonzi et al. 2017). Our data suggest that D1DR+ neurons respond to this phasic dopaminergic release early in the interval and initiate temporal processing via delta-range coherence with MFC ramping neurons. About 2-Hz stimulation may be effective, in part, because it resonates with this delta/theta coherence in MFC.

Our findings go beyond correlative evidence as we show that MFC D1DR+ stimulation improves interval timing (Narayanan et al. 2012; Kim et al. 2017; Parker et al. 2017). This is only true when mesocortical dopamine circuits are disrupted, leading to less task-related MFC delta/theta power (Parker, Chen, et al. 2014; Kim et al. 2017). Stimulation is not consistently effective in animals with intact mesocortical dopamine circuits, likely because dopaminergic circuits are close to optimal network function (Vijayraghavan et al. 2007; Cools and D'Esposito 2011; Narayanan, Rodnitzky, et al. 2013; Kim et al. 2017). Our previous stimulation protocols delivered delta stimulation of D1DR+ neurons at a consistent phase during the entire interval (Narayanan et al. 2012; Kim et al. 2017; Parker et al. 2017). If MFC D1DR+ neurons exhibited time-related ramping, this stimulation would have further disrupted interval timing by replacing a time-dependent signal (ramping) with a time-independent signal (a constant 2-Hz firing rate over the interval). We found that constant stimulation of MFC D1DR+ neurons both created time-related ramping among untagged MFC neurons and improved interval-timing behavior (Kim et al. 2017). Findings in Fig. 5B,F indicate that delta coherence phase-locked to the cue and early

in the interval is sufficient to produce the effects of MFC D1DR+ neuron stimulation on behavior. Notably, in this study and in other work from our group in mice, rats, and humans (Kim et al. 2017; Parker et al. 2017; Kelley et al. 2018), stimulation at higher frequencies did not reliably affect behavior. One reason may be that higher-frequency stimulation did not engage delta/theta activity among MFC neurons, which may be key for cognitive control (Cavanagh and Frank 2014). Furthermore, stimulating early versus late in the interval with identical length of stimulation and number of pulses produced differential effects on behavior (Fig. 6B). Finally, brain stimulation at delta frequencies can entrain delta rhythms (Kelley et al. 2018; Kim et al. 2017). These data indicate that our behavioral effects are not a result of generalized activation on the MFC. Rather, our findings indicate that there is delta/theta coherence between MFC D1DR+ neurons and ramping neurons, and that specifically increasing coherence at delta/theta frequencies via optogenetic stimulation can improve interval timing in dopamine-depleted animals.

These data support a role for oscillatory activity in temporal encoding, as predicted by the striatal beat-frequency model of timing (Matell and Meck 2004; Meck et al. 2008). This model predicts that the degree of phase-locking between neurons can reflect elapsed time (Buhusi and Meck 2005). Delta coherence in Fig. 5 implies that oscillatory structure early in temporal intervals might be a meaningful temporal signal among MFC neurons. It may be that the animal is only timing until the initiate responding. Indeed, the first response times occur around this transition in coherence in Fig. 5A. MFC D1DR+ interactions may help initiate drift–diffusion dynamics that encode time (Simen et al. 2011) via ramping or other mechanisms (Matell and Meck 2004; Latimer et al. 2015; Narayanan 2016). Also of interest is that PC4 seems to highly load on MFC D1DR+ neurons, and this component has oscillatory features with a period of approximately 6 s. This may be related to low-frequency delta rhythms, or a signature of oscillations playing a role in temporal computations. This idea is difficult to test in our single fixed-interval task; but tasks with peak trials and multiple intervals might provide insight into the significance of this type of activity.

Interval timing requires many complex processes that involve MFC, such as waiting and inhibitory control over inappropriate actions (Hardung et al. 2017; Narayanan and Laubach 2017). Some of these signals may be encoded by neurons with time-related ramps (see PC1 in Narayanan and Laubach 2009). As the interval end approaches, less waiting and self-control is required, facilitating goal-directed movements (Narayanan 2016). Our prior work has shown that delta/theta rhythms can flexibly and adaptively engage MFC neurons in service of cognitive control (Narayanan, Cavanagh et al. 2013; Laubach et al. 2015).

D1DRs play a critical role in working memory in lateral prefrontal regions in primates (Sawaguchi and Goldman-Rakic 1991, 1994; Williams and Goldman-Rakic 1995; Goldman-Rakic et al. 2004), which are distinct from rodent MFC (Preuss 1995; Narayanan and Laubach 2017). Our group has shown that MFC D1DR+ is critically required for timing behaviors (Narayanan et al. 2012; Parker, Alberico, et al. 2013) and time-related ramping among MFC neurons (Parker, Narayanan, et al. 2014; Parker, Ruggiero, et al. 2015), but it remains to be seen how these insights relate to other tasks involving cognitive control and prefrontal brain areas in other species.

Dopamine plays a key role in interval timing (Malapani et al. 1998; Meck 2006; Coull et al. 2011). Dopamine may critically modulate temporal judgments, with inhibiting dopamine neurons slowing down time estimation and stimulating dopamine neurons speeding up time estimation (Soares et al. 2016). This group targeted nigrostriatal dopamine neurons, whereas the cortex receives input from the VTA (Williams and Goldman-Rakic 1998; Alberico et al. 2015). Several studies from our group indicate that cortical dopamine is involved in the accuracy of timing (Narayanan et al. 2012; Parker, Chen, et al. 2014; Parker, Ruggiero, et al. 2015; Kim et al. 2017) perhaps as a function of impaired inhibitory control (Narayanan et al. 2006; Parker, Alberico, et al. 2013; Narayanan and Laubach 2017). Both cortical and striatal processes may be at work in patients with Parkinson's disease and schizophrenia (Malapani et al. 1998; Ward et al. 2012; Nombela et al. 2016). Studying these circuits in tandem as a function of dopaminergic signaling may shed light on these questions.

We find that MFC D1DR+ neurons have less ramping activity and less motor-related modulation, although they have equivalent cue-modulation to other MFC neurons. This may suggest that these neurons are less task-responsive, in part because they are engaged by delta/theta rhythms that instantiate cognitive control (Parker, Chen, et al. 2014; Parker, Ruggiero, et al. 2015). Our working model is that MFC D1DR+ neurons are specifically tuned to these rhythms that indicate key moments in the task—such as the instructional cue—and help engage MFC ramping neurons involved in temporal control of action. Future studies might test this idea by investigating the role of MFC D1DR+ in tasks with more elaborate cognitive processing, such as working memory.

Our study is limited in making anatomical inferences because we cannot directly visualize recorded neurons and their connectivity. Additionally, we cannot further describe untagged MFC neurons, although they appear to have the strongest ramping activity. Prefrontal neurons are densely and recurrently connected via local microcircuits and distant projections (Constantinidis et al. 2001; Han et al. 2017). Because of technical limitations, we cannot specify the exact pathway by which MFC D1DR+ neurons entrain ramping neurons or the synaptic connectivity patterns of MFC D1DR+ neurons to other MFC neurons. Such insights likely require correlation of optogenetic approaches with techniques that have better spatial resolution, such as two-photon imaging. It is not clear, however, if these techniques can detect delta/theta coherence (Chen et al. 2013). A major technical limitation is that because of our recording and sorting approach, our recordings are biased towards large pyramidal cells and thus we cannot reliably record from cortical interneurons. This point is particularly important because MFC D1DRs can be expressed on interneurons as well as pyramidal cells (Muly et al. 1998; Trantham-Davidson et al. 2008; Glausier et al. 2009). Designing mice with Cre targeted to D1DR+ interneurons versus pyramidal cells, or tetrode/intracellular/juxtacellular recording techniques might be better able to address the role of MFC D1DR+ pyramidal neurons versus interneurons. A further limitation is that our analysis of ramping might be influenced by averaging over multiple trials (Latimer et al. 2015). Despite these limitations, our results provide novel insight into how dopamine influences cognitive processing in frontal circuits, which could have relevance for disorders such as Parkinson's disease and schizophrenia.

Funding

This work was supported by National Institute of Neurological Disorders and Stroke (R01 NS078100/K08 NS078100), National Institute of Mental Health, and NARSAD Young Investigator Grant from Brain and Behavior Research Foundation (grant No. 2014/22817-1).

Notes

We would like to thank Eric Emmons and Ben De Corte for feedback on this manuscript, and Sangwoo Han for technical assistance. *Conflict of Interest*: None declared.

References

Abi-Dargham A, Mawlawi O, Lombardo I, Gil R, Martinez D, Huang Y, Hwang D-R, Keilp J, Kochan L, Van Heertum R, et al. 2002. Prefrontal dopamine D1 receptors and working memory in schizophrenia. J Neurosci. 22:3708–3719.

Alberico SL, Cassell MD, Narayanan NS. 2015. The vulnerable ventral tegmental area in Parkinson's disease. Basal Ganglia. 5:51–55.

Aoi MC, Lepage KQ, Kramer MA, Eden UT. 2015. Rate-adjusted spike-LFP coherence comparisons from spike-train statistics. J Neurosci Methods. 240:141–153.

Buhusi CV, Meck WH. 2005. What makes us tick? Functional and neural mechanisms of interval timing. Nat Rev Neurosci. 6:755–765.

Cardin JA, Carlén M, Meletis K, Knoblich U, Zhang F, Deisseroth K, Tsai L-H, Moore CI. 2009. Driving fast-spiking cells induces gamma rhythm and controls sensory responses. Nature. 459:663–667.

Cavanagh JF, Frank MJ. 2014. Frontal theta as a mechanism for cognitive control. Trends Cogn Sci (Regul Ed). 18:414–421.

Cavanagh JF, Zambrano-Vazquez L, Allen JJB. 2012. Theta lingua franca: a common mid-frontal substrate for action monitoring processes. Psychophysiol. 49:220–238.

Chapin JK, Nicolelis MA. 1999. Principal component analysis of neuronal ensemble activity reveals multidimensional somatosensory representations. J Neurosci Methods. 94:121–140.

Chen K-H, Okerstrom KL, Kingyon JR, Anderson SW, Cavanagh JF, Narayanan NS. 2016. Startle habituation and midfrontal theta activity in Parkinson's disease. J Cogn Neurosci. 12: 1923–1932.

Chen T-W, Wardill TJ, Sun Y, Pulver SR, Renninger SL, Baohan A, Schreiter ER, Kerr RA, Orger MB, Jayaraman V, et al. 2013. Ultrasensitive fluorescent proteins for imaging neuronal activity. Nature. 499:295–300.

Constantinidis C, Franowicz MN, Goldman-Rakic PS. 2001. Coding specificity in cortical microcircuits: a multiple-electrode analysis of primate prefrontal cortex. J Neurosci. 21:3646–3655.

Cools R, D'Esposito M. 2011. Inverted-U-shaped dopamine actions on human working memory and cognitive control. Biol Psychiatry. 69:e113–e125.

Coull JT, Cheng R-K, Meck WH. 2011. Neuroanatomical and neurochemical substrates of timing. Neuropsychopharmacology. 36:3–25.

Emmons EB, Corte BJD, Kim Y, Parker KL, Matell MS, Narayanan NS. 2017. Rodent medial frontal control of temporal processing in the dorsomedial striatum. J Neurosci. 37:8718–8733.

Emmons EB, Ruggiero RN, Kelley RM, Parker KL, Narayanan NS. 2016. Corticostriatal field potentials are modulated at delta and theta frequencies during interval-timing task in rodents. Front Psychol. 7:459.

Fonzi KM, Lefner MJ, Phillips PEM, Wanat MJ. 2017. Dopamine encodes retrospective temporal information in a context-independent manner. Cell Rep. 20:1765–1774.

Fry W, Kelleher RT, Cook L. 1960. A mathematical index of performance on fixed-interval schedules of reinforcement. J Exp Anal Behav. 3:193–199.

Fuster J. 2008. The Prefrontal Cortex. 4th ed. New York, NY: Academic Press.

Gaspar P, Bloch B, Le Moine C. 1995. D1 and D2 receptor gene expression in the rat frontal cortex: cellular localization in different classes of efferent neurons. Eur J Neurosci. 7: 1050–1063.

Glausier JR, Khan ZU, Muly EC. 2009. Dopamine D1 and D5 receptors are localized to discrete populations of interneurons in primate prefrontal cortex. Cereb Cortex. 19:1820–1834.

Goldman-Rakic PS, Castner SA, Svensson TH, Siever LJ, Williams GV. 2004. Targeting the dopamine D1 receptor in schizophrenia: insights for cognitive dysfunction. Psychopharmacology (Berl). 174:3–16.

Gouvea TS, Monteiro T, Motiwala A, Soares S, Machens C, Paton JJ. 2015. Striatal dynamics explain duration judgments. eLife. 4.pii: e11386.

Han S-W, Kim Y-C, Narayanan NS. 2017. Projection targets of medial frontal D1DR-expressing neurons. Neurosci Lett. 655: 166–171.

Hardung S, Epple R, Jackel Z, Eriksson D, Uran C, Senn V, Gibor L, Yizhar O, Diester I. 2017. A functional gradient in the rodent prefrontal cortex supports behavioral inhibition. Curr Biol. 27:549–555.

Jenni NL, Larkin JD, Floresco SB. 2017. Prefrontal dopamine D1 and D2 receptors regulate dissociable aspects of decision-making via distinct ventral striatal and amygdalar circuits. J Neurosci. 37(26):6200–6213.

Kelley R, Flouty O, Emmons EB, Kim Y, Kingyon J, Wessel JR, Oya H, Greenlee JD, Narayanan NS. 2018. A human prefrontal-subthalamic circuit for cognitive control. Brain. 141(1):205–216.

Kim J, Ghim J-W, Lee JH, Jung MW. 2013. Neural correlates of interval timing in rodent prefrontal cortex. J Neurosci. 33: 13834–13847.

Kim Y-C, Han S-W, Alberico SL, Ruggiero RN, De Corte B, Chen K-H, Narayanan NS. 2017. Optogenetic stimulation of frontal D1 neurons compensates for impaired temporal control of action in dopamine-depleted mice. Curr Biol. 27:39–47.

Land BB, Narayanan NS, Liu R-J, Gianessi CA, Brayton CE, Grimaldi DM, Sarhan M, Guarnieri DJ, Deisseroth K, Aghajanian GK, et al. 2014. Medial prefrontal D1 dopamine neurons control food intake. Nat Neurosci. 17:248–253.

Latimer KW, Yates JL, Meister MLR, Huk AC, Pillow JW. 2015. NEURONAL MODELING. Single-trial spike trains in parietal cortex reveal discrete steps during decision-making. Science. 349:184–187.

Laubach M, Caetano MS, Narayanan NS. 2015. Mistakes were made: neural mechanisms for the adaptive control of action initiation by the medial prefrontal cortex. Journal of Physiology-Paris. 109(1–3):104–117.

Ma L, Hyman JM, Phillips AG, Seamans JK. 2014. Tracking progress toward a goal in corticostriatal ensembles. J Neurosci. 34:2244–2253.

Malapani C, Rakitin B, Levy R, Meck WH, Deweer B, Dubois B, Gibbon J. 1998. Coupled temporal memories in Parkinson's disease: a dopamine-related dysfunction. J Cogn Neurosci. 10:316–331.

Matell MS, Meck WH. 2004. Cortico-striatal circuits and interval timing: coincidence detection of oscillatory processes. Brain Res Cogn Brain Res. 21:139–170.

Meck WH. 2006. Neuroanatomical localization of an internal clock: a functional link between mesolimbic, nigrostriatal, and mesocortical dopaminergic systems. Brain Res. 1109: 93–107.

Meck WH, Penney TB, Pouthas V. 2008. Cortico-striatal representation of time in animals and humans. Curr Opin Neurobiol. 18:145–152.

Miller BT, D'Esposito M. 2005. Searching for "the top" in top-down control. Neuron. 48:535–538.

Mitra P, Bokil H. 2008. Observed brain dynamics. Oxford; New York: Oxford University Press.

Muly EC 3rd, Szigeti K, Goldman-Rakic PS. 1998. D1 receptor in interneurons of macaque prefrontal cortex: distribution and subcellular localization. J Neurosci. 18:10553–10565.

Narayanan NS. 2016. Ramping activity is a cortical mechanism of temporal control of action. Curr Opin Behav Sci. 8: 226–230.

Narayanan NS, Cavanagh JF, Frank MJ, Laubach M. 2013. Common medial frontal mechanisms of adaptive control in humans and rodents. Nat Neurosci. 16:1888–1897.

Narayanan NS, Horst NK, Laubach M. 2006. Reversible inactivations of rat medial prefrontal cortex impair the ability to wait for a stimulus. Neuroscience. 139:865–876.

Narayanan NS, Land BB, Solder JE, Deisseroth K, DiLeone RJ. 2012. Prefrontal D1 dopamine signaling is required for temporal control. Proc Natl Acad Sci USA. 109:20726–20731.

Narayanan NS, Laubach M. 2009. Delay activity in rodent frontal cortex during a simple reaction time task. J Neurophysiol. 101:2859–2871.

Narayanan NS, Laubach M. 2017. Inhibitory control: mapping medial frontal cortex. Curr Biol. 27:R148–R150.

Narayanan NS, Rodnitzky RL, Uc EY. 2013. Prefrontal dopamine signaling and cognitive symptoms of Parkinson's disease. Rev Neurosci. 24:267–278.

Niki H, Watanabe M. 1979. Prefrontal and cingulate unit activity during timing behavior in the monkey. Brain Res. 171: 213–224.

Nombela C, Wolpe N, Barker RA, Rowe JB. 2016. Time on timing: dissociating premature responding from interval sensitivity in Parkinson's disease. Mov Disord. 31:1163–1172.

Okubo Y, Suhara T, Suzuki K, Kobayashi K, Inoue O, Terasaki O, Someya Y, Sassa T, Sudo Y, Matsushima E, et al. 1997. Decreased prefrontal dopamine D1 receptors in schizophrenia revealed by PET. Nature. 385:634–636.

Parker KL, Alberico SL, Miller AD, Narayanan NS. 2013. Prefrontal D1 dopamine signaling is necessary for temporal expectation during reaction time performance. Neuroscience. 255:246–254.

Parker KL, Andreasen NC, Liu D, Freeman JH, O'Leary DS. 2013. Eyeblink conditioning in unmedicated schizophrenia patients: a positron emission tomography study. Psychiatry Res. 214(3):402–409.

Parker KL, Chen K-H, Kingyon JR, Cavanagh JF, Narayanan NS. 2014. D1-dependent 4 Hz oscillations and ramping activity in rodent medial frontal cortex during interval timing. J Neurosci. 34:16774–16783.

Parker KL, Chen K-H, Kingyon JR, Cavanagh JF, Naryanan NS. 2015. Medial frontal ~4 Hz activity in humans and rodents is attenuated in PD patients and in rodents with cortical dopamine depletion. J Neurophysiol. 114(2):1310–1320.

Parker KL, Kim Y-C, Kelley RM, Nessler AJ, Chen K-H, Muller-Ewald VA, Andreasen NC, Narayanan NS. 2017. Delta-frequency stimulation of cerebellar projections can compensate for schizophrenia-related medial frontal dysfunction. Mol Psychiatry. 22(5):647–655.

Parker KL, Narayanan NS, Andreasen NC. 2014. The therapeutic potential of the cerebellum in schizophrenia. Front Syst Neurosci. 8:163.

Parker KL, Ruggiero RN, Narayanan NS. 2015. Infusion of D1 Dopamine Receptor Agonist into Medial Frontal Cortex Disrupts Neural Correlates of Interval Timing. Front Behav Neurosci. 9:294.

Preuss T. 1995. Do rats have prefrontal cortex? The Rose–Woolsey–Akert program reconsidered. J Cogn Neurosci. 7:1–24.

Sawaguchi T, Goldman-Rakic PS. 1991. D1 dopamine receptors in prefrontal cortex: involvement in working memory. Science. 251:947–950.

Sawaguchi T, Goldman-Rakic PS. 1994. The role of D1-dopamine receptor in working memory: local injections of dopamine antagonists into the prefrontal cortex of rhesus monkeys performing an oculomotor delayed-response task. J Neurophysiol. 71:515–528.

Schultz W. 1997. Dopamine neurons and their role in reward mechanisms. Curr Opin Neurobiol. 7:191–197.

Simen P, Balci F, de Souza L, Cohen JD, Holmes P. 2011. A model of interval timing by neural integration. J Neurosci. 31: 9238–9253.

Soares S, Atallah BV, Paton JJ. 2016. Midbrain dopamine neurons control judgment of time. Science. 354:1273–1277.

St Onge JR, Abhari H, Floresco SB. 2011. Dissociable contributions by prefrontal D1 and D2 receptors to risk-based decision making. J Neurosci. 31:8625–8633.

Trantham-Davidson H, Kroner S, Seamans JK. 2008. Dopamine modulation of prefrontal cortex interneurons occurs independently of. Cereb Cortex. 18:951–958.

Vijayraghavan S, Wang M, Birnbaum SG, Williams GV, Arnsten AFT. 2007. Inverted-U dopamine D1 receptor actions on prefrontal neurons engaged in working memory. Nat Neurosci. 10:376–384.

Ward RD, Kellendonk C, Kandel ER, Balsam PD. 2012. Timing as a window on cognition in schizophrenia. Neuropharmacology. 62(3):1175–1181.

Williams GV, Goldman-Rakic PS. 1995. Modulation of memory fields by dopamine D1 receptors in prefrontal cortex. Nature. 376:572–575.

Williams SM, Goldman-Rakic PS. 1998. Widespread origin of the primate mesofrontal dopamine system. Cereb Cortex. 8: 321–345.

Xu M, Zhang S, Dan Y, Poo M. 2014. Representation of interval timing by temporally scalable firing patterns in rat prefrontal cortex. Proc Natl Acad Sci USA. 111:480–485.